International Journal of Trend in Scientific Research and Development (IJTSRD)
Volume 7 Issue 4, July-August 2023 Available Online: www.ijtsrd.com e-ISSN: 2456 – 6470

An Integrated Approach of ACM and CDMA in a Novel Multi-User Spatial Modulation Scheme

Kumari Kanchana[1], Dr. Prabhat Sharma[2]

[1]M Tech Scholar, Department of Electronics and Communication Engineering,
[2]Research Guide, Department of Electronics and Communication Engineering,
[1,2]Oriental Institute of Science and Technology, Bhopal, Madhya Pradesh, India

ABSTRACT

The research focus in wireless communication access technologies is driven by the demand for high peak data rates and significantly improved spectral efficiencies, as well as the support for specific quality of service (QoS) requirements. By leveraging the orthogonality of space constellations and signal constellations, well-established digital signal modulation schemes can be employed. The spatial multiplexing gain is achieved through the concurrent transmission of spatially encoded bits. This thesis investigates and compares the analytical and numerical performance of Spatial Modulation (SM) under various channel conditions, taking into account practical channel considerations, in comparison to existing MIMO techniques. The results demonstrate that SM achieves a low bit error ratio (BER) while substantially reducing receiver complexity, all while maintaining spectral efficiency.

KEYWORDS: *MIMO, Spatial Modulation, BER, Bit Error Rate, Modulation Technique etc.*

How to cite this paper: Kumari Kanchana | Dr. Prabhat Sharma "An Integrated Approach of ACM and CDMA in a Novel Multi-User Spatial Modulation Scheme" Published in International Journal of Trend in Scientific Research and Development (ijtsrd), ISSN: 2456-6470, Volume-7 | Issue-4, August 2023, pp.220-228, URL: www.ijtsrd.com/papers/ijtsrd59660.pdf

IJTSRD59660

Copyright © 2023 by author (s) and International Journal of Trend in Scientific Research and Development Journal. This is an Open Access article distributed under the terms of the Creative Commons Attribution License (CC BY 4.0) (http://creativecommons.org/licenses/by/4.0)

I. INTRODUCTION

The rise of wireless communication systems like vehicle-to-vehicle (V2V) communication [1] and wireless high-definition (HD) television has stimulated research in MIMO technology. MIMO has emerged as a key technique for enhancing data throughput, link reliability, and spectral efficiency [2-4]. MIMO techniques can be broadly categorized into spatial diversity and spatial multiplexing schemes. Spatial diversity techniques [5, 6] enhance link reliability by transmitting multiple redundant copies of data over independent channels to the receiver. Alamouti's scheme [6] is a popular transmit diversity technique that utilizes a pair of transmit antennas to achieve complete transmit diversity. However, this approach trades diversity gains for low spectral efficiency, which remains unchanged compared to a single-input multiple-output (SIMO) system [7].

Among the various existing technologies, multiple-input multiple-output (MIMO) with adaptive coding and modulation holds promise as a candidate for future wireless systems. MIMO systems enhance spectral efficiency by utilizing multiple transmit antennas to simultaneously transmit data to the receiver. Adaptive modulation and coding enable robust and efficient transmission over channels that vary over time. The fundamental principle is to estimate the channel at the receiver and provide this estimate as feedback to the transmitter, allowing the transmission scheme to adapt to the channel characteristics. The concept involves treating the transmit antenna array as a spatial constellation diagram, where the actual antennas serve as constellation points. Each spatial constellation point is mapped to a distinct bit sequence. At any given moment, only one antenna transmits energy, and the relevant information is encoded in the physical location of the transmitting antenna or spatial constellation point. Naturally, this necessitates a

novel detection process at the receiver, known as antenna detection.

RELATED WORK

Space shift keying (SSK) modulation in [28] can be regarded as a specific instance of Spatial Modulation (SM), where only the transmit antenna indices convey information. The SSK scheme eliminates the need for conventional modulation techniques, reducing receiver complexity compared to SM while maintaining performance gains. Similar to SM, SSK schemes are limited to a number of transmit antennas that are a power of two. When the transmit antenna constraint cannot be met, the generalized SSK (GSSK) scheme [29] offers a viable solution. In [29], GSSK utilizes combinations of antenna indices to transmit information, allowing for application to any antenna configuration. However, the flexibility of GSSK comes at the cost of reduced performance compared to SSK [29].

Fractional bit encoded spatial modulation (FBE-SM) in [30] represents a more versatile SM scheme based on modulus conversion theory. The FBE-SM approach enables the transmitter to operate with an arbitrary number of antennas, making it suitable for compact mobile devices with limited space for transmit antennas. Numerical results demonstrate that FBE-SM provides design flexibility and the necessary degrees of freedom to balance performance and capacity [30].

Trellis coded spatial modulation (TCSM) in [31] incorporates trellis coded modulation (TCM) into the antenna constellation points of SM. This increases the distance between antenna constellation points, leading to improved performance over spatially correlated channels. The TCSM scheme is analyzed in [32], which proposes an analytical framework for performance evaluation over correlated fading channels.

Soft-output maximum likelihood (ML) detection in [33] introduces a soft-output ML detector for SM orthogonal frequency division multiplexing (OFDM) systems, surpassing the performance of conventional hard decision-based SM detectors.

SM with partial channel state information (CSI) at the receiver in [34] develops and analyzes an SM detector with an unknown phase reference at the receiver. Monte Carlo simulations validate the analytical frameworks and investigate the performance of the proposed detector. Results highlight the severe degradation of SM performance when phase information is unavailable at the receiver, emphasizing the importance of accurate channel estimation for efficient SM operation [34].

Optical spatial modulation (OSM) in [35] is an indoor optical wireless communication technique based on SM. The OSM scheme achieves double and quadruple the data rate compared to conventional on-off keying and pulse-position modulation techniques, respectively [35]. In [36], channel coding is applied to OSM, and the bit error rate (BER) performance of both hard and soft detectors is analyzed analytically. Monte Carlo simulation results demonstrate that the application of channel coding techniques enhances OSM performance by approximately 5dB and 7dB for hard and soft decisions, respectively [36].

Normalized maximum ratio combining (NMRC) detector in [37] proposes a low-complexity sub-optimal SM detection algorithm for unconstrained channels. Additionally, an antenna index (AI) list-based detector is introduced [37]. Monte Carlo simulation results and analysis indicate that the AI list-based scheme achieves near-optimal performance with reduced complexity compared to the optimal SM detector. However, the AI list-based detector operates efficiently only for list sizes equal to half the number of transmit antennas, resulting in a 40% increase in complexity compared to the NMRC scheme.

Space-time block coded spatial modulation (STBC-SM) in [38] combines SM and STBC to exploit the transmit diversity potential of MIMO channels. The proposed scheme is analyzed in [38], deriving a closed-form expression for the average BER. Monte Carlo simulation results support the analytical frameworks and demonstrate the performance advantages of STBC-SM over SM. Results indicate that STBC-SM offers performance enhancements of 3dB-5dB (depending on spectral efficiency) compared to conventional SM [38]. It should be noted that a similar scheme termed Alamouti coded spatial modulation is proposed in this dissertation; however, both schemes have been independently developed based on different paradigms employed.

II. SPATIAL MODULATION

In this section, we commence by introducing the SM–MIMO concept, illustrating it with the aid of some simple examples. Again, we denote by Nt and Nr the number of TAs and RAs, respectively. The cardinality of the signal constellation diagram is denoted by M. Either PSK or QAM are considered. In general, Nt, Nr, and M can be chosen independently of each other. At the receiver, optimum ML demodulation is considered. Thus, Nr can be chosen independently of Nt . For ease of exposition, we assume $N_t = 2^{n_t}$ and $M = 2^m$ with nt and m being two positive integers. In Section IV, we describe general SM–MIMO encodings as well as some suboptimal (non-ML) demodulation schemes.

In Fig. 1, the SM–MIMO concept is illustrated for Nt = M = 2, and it is compared to the conventional SMX scheme and the OSTBC scheme designed for transmit diversity. In the latter case, the Alamouti scheme is considered as an example [80].

In SMX–MIMO, two PSK/QAM symbols (S1 and S2) are simultaneously transmitted from a pair of TAs in a single channel use. For arbitrary Nt and M, the rate of SMX is $R_{SMX} = N_t log_2(M)$bpcu.

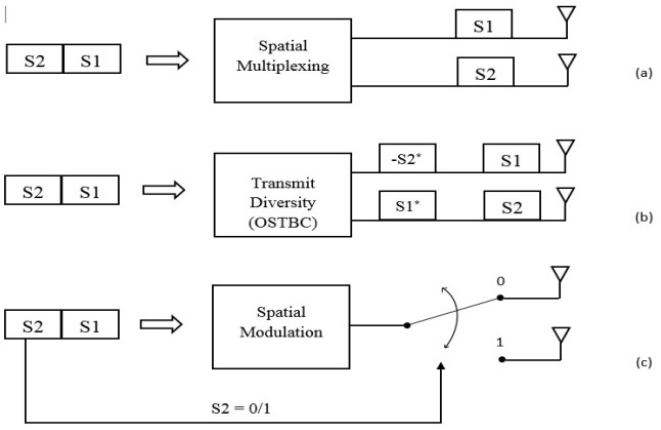

Figure 1 Illustration of three MIMO concepts: (a) spatial multiplexing; (b) transmit diversity; and (c) SM.

In OSTBC–MIMO, two PSK/QAM symbols (S1 and S2) are first encoded and then simultaneously transmitted from a pair of TAs in two channel uses. For arbitrary Nt and M, the rate of OSTBC is $R_{OSTBC} = R_c log_2(M)$bpcu, where $R_c = N_M/N_{cu} \leq 1$ is the rate of the space-time block code and NM is the number of information symbols transmitted in Ncu channel uses If, as shown in Fig. 1, the Alamouti code is chosen, then we have Rc = 1.

In SM–MIMO, only one (S1) out of the two symbols is explicitly transmitted, while the other symbol (S2) is implicitly transmitted by determining the index of the active TA in each channel use. In other words, in SM–MIMO, the information symbols are modulated onto two information carrying units: a) one PSK/QAM symbol; and b) a single active TA via an information-driven antenna-switching mechanism. For arbitrary Nt and M, the rate of SM is $R_{SM} = log_2(M) + log_2(N_t)$ bpcu [76], [82].

In Figs. 2 and 3, the encoding mechanism of SM–MIMO is illustrated for Nt = M= 4 by considering two generic channel uses, where the concept of ‘‘SM or spatialconstellation diagram’’ is also introduced. The rate of this MIMO setup is $R_{SM} = log_2(M) + log_2(N_t) = 4$ bpcu, hence the encoder processes the information bits in blocks of four bits each. In the first channel use shown in Fig. 2, the block of bits to be encoded is ‘‘1100.’’ The first $log_2(N_t) = 2$bits, ‘‘11,’’ determine the single active TA (TX3), while the second$log_2(M) = 2$ bits, ‘‘00,’’ determine the transmitted PSK/QAM symbol. Likewise, in thesecond channel use shown in Fig. 3, the block of bits to be encoded is ‘‘0001.’’ The first $log_2(N_t) = 2$bits, ‘‘00,’’ determine the single active TA (TX0), while the second $log_2(M) = 2$ bits, ‘‘01,’’ determine the transmitted PSK/ QAM symbol.

The activated TA may change every channel use according to the input information bits. Thus, TA switching is an effective way of mapping the information bits to TA indices and of increasing the transmission rate. It is worth mentioning here that the idea of increasing the rate of wireless communications using TA switching has been alluded in pioneering MIMO papers under the concept of ‘‘spatial cycling using one transmitter at a time’’.

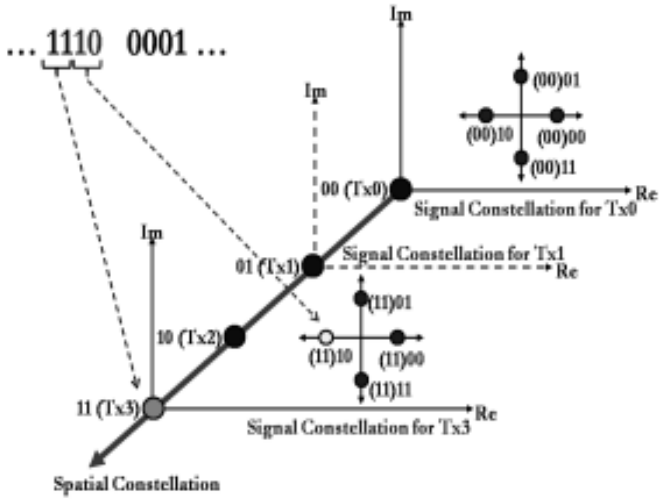

Figure 2 Illustration of the 3-D encoding of SM (first channel use).

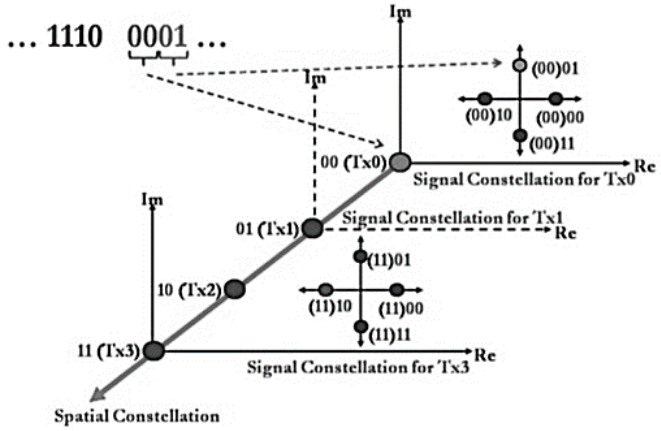

Figure 3 Illustration of the 3-D encoding of SM (second channel use).

The information bits are modulated onto a 3-D constellation diagram, which generalizes the known 2-D (complex) signal-constellation diagram of PSK/QAM modulation schemes. The thirddimension is provided by the antenna array, where some of the bits are mapped to the TAs. In SM–MIMO research, this third dimension is termed the ‘‘spatial-constellation diagram’’ [76]. In simple mathematical

terms, the signal model of SM– MIMO, assuming a frequency-flat channel model, is as follows:

$\mathbf{y} = \mathbf{Hx} + \mathbf{n}$ where $\mathbf{y} \in \mathbb{C}^{N_r \times 1}$ is the complex received vector; $\mathbf{H} \in \mathbb{C}^{N_r \times N_t}$ is the complex channel matrix; $\mathbf{n} \in \mathbb{C}^{N_r \times 1}$is the complex AWGN at the receiver; and $\mathbf{x} = \mathbf{e}s \in \mathbb{C}^{N_t \times 1}$ is the complex modulated vector with $s \in \mathbb{S} \subseteq \mathbb{C}^{1 \times 1}$ being the complex (scalar) PSK/QAM modulated symbol belonging to the signal-constellation diagram and $\mathbf{e} \in \mathcal{A}$ being the Nt×1 vector belonging to the spatial-constellation diagram $\mathcal{A}$ as follows:

$$\mathbf{e}_t = \begin{cases} 1, \text{if the tth TA is active} \\ 0, \text{if the tth TA is not active} \end{cases}$$

where et is the tth entry of e for t = 1, 2,...,Nt. In other words, the points (Nt-dimensional vectors) of the spatialconstellation diagram are the Nt unit vectors of the natural basis of the Nt-dimensional Euclidean space.

If Nt = 1, SM–MIMO reduces to conventional singleantenna communications, where the information bits are encoded only onto the signal-constellation diagram. In this case, the rate is $R_0 = log_2(M)$. On the other hand, if M = 1 the information is encoded only onto the spatial-constellationdiagrambyproviding etequalto $R_{SSK} = log_2(N_t)$. In particular, SSK modulation is a MIMO scheme, where data transmission takes place only through the informationdriven TA switching mechanism. It is apparent that SM– MIMO can be viewed as the combination of single-antenna PSK/QAM and SSK–MIMO modulations.

III. PROPOSED METHODOLOGY

Figure 4 illustrates the system model of the proposed two-user multiple access spatial modulation (MA-SM) system with adaptive modulation and coding (AMC). The system comprises a multiple-input multiple-output (MIMO) wireless link. Within this setup, two user transmitters transmit their signals through a Rayleigh fading channel to a shared receiver. The receiver, equipped with a spatial modulation (SM) demodulator and a maximum likelihood (ML) detector as described in the previous section, plays a crucial role. It computes the joint probability of the two received signals and employs the ML detector to calculate the Euclidean distance between the received vector signal and the set of all possible received signals. The ML detector then selects the closest signal based on this distance calculation..

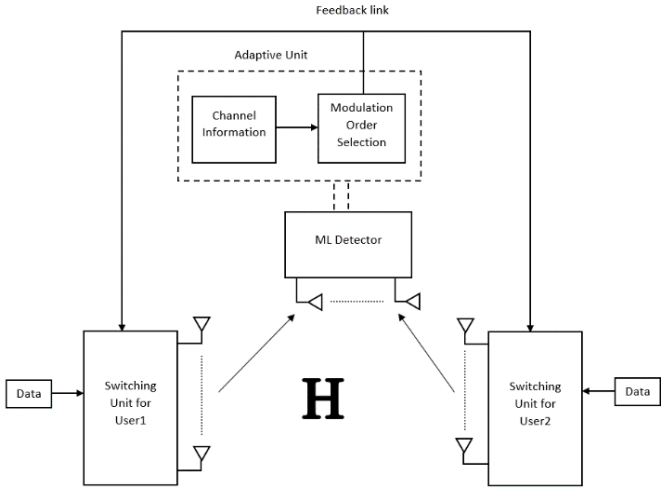

Figure 4. 2-user Multiple Access Spatial Modulation with ACM System Model

In contrast to conventional spatial modulation (SM), which assigns the same modulation order for data mapping across all transmit antennas, the proposed scheme introduces a switching unit at the user end. This switching unit dynamically selects modulation orders for each transmit antenna. Specifically, when the channel exhibits slow variations, the adaptive unit at the receiver calculates the optimal modulation candidate for transmission and communicates this information to the two users through a low-bandwidth feedback path. Subsequently, the transmitters utilize the assigned modulation orders for the subsequent channel usage.

The adaptive unit utilizes the channel state information obtained by the receiver to determine the optimal level of modulation. This information is then relayed back to the transmitters of both users, who adjust their modulation schemes accordingly for the next transmitted signal. If the channel conditions change, the modulation order is also adjusted. This adaptation is achieved by predefining a minimum and maximum bit error rate (BER) threshold. The receiver compares the BER of the received signal with these pre-set values. If the BER is lower than the desired threshold, the frame size of the transmitted signal can be increased. Conversely, if the BER is higher than the desired threshold, the frame size of the transmitted signal is reduced. The ultimate goal is to optimize the utilization of the available channel bandwidth. Depending on the channel's requirements and characteristics, the transmitter dynamically adapts itself to the most suitable modulation scheme, ensuring a desired BER for improved spectral efficiency.

IV. SIMULATION AND RESULTS

In this particular section, our focus lies on the examination and comparison of graphs obtained under different levels of channel attenuation, both with and without adaptive coding and modulation

(ACM). Each presented simulation graph encompasses four distinct results. The pink and cyan graphs represent the outcomes of a two-user multiple access spatial modulation system without ACM, while the red and blue graphs showcase the results obtained using our proposed methodology with ACM.

Throughout the subsequent section, we delve into the exploration of diverse variations in the simulation results achieved by manipulating the channel attenuation of the system. This alteration in channel attenuation impacts the channel state information (CSI) and illustrates the functioning of adaptive modulation. The graphs primarily investigate the bit error rate (BER) of the system relative to the signal-to-noise ratio (SNR) in dB of the proposed scheme. The ultimate objective, as previously stated, is to minimize the BER of the received signal, which becomes strikingly evident upon mere observation of the graphs.

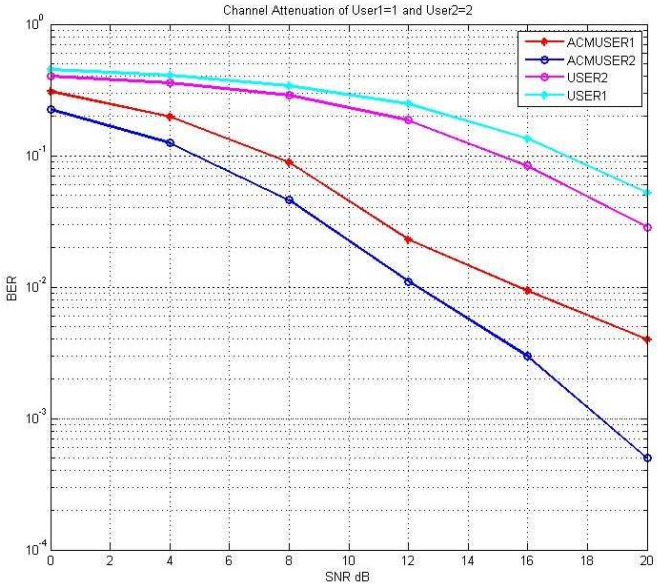

Figure 5 Comparison Results for users 1 and 2 with and without ACM and channel attenuation of 1 and 2 dB respectively.

The depicted graph showcases the behavior of signals with and without adaptive coding and modulation (ACM), where User1 and User2 possess channel attenuations of 1 and 2, respectively. In the graph without ACM, which solely employs multiple access spatial modulation, the bit error rate (BER) is higher. While it gradually decreases with the signal-to-noise ratio (SNR), it does not go below 0.001. Conversely, in the presence of ACM, the BER follows a more linear trend and sharply declines towards predefined lower bound values. These upper and lower bound values are predetermined to keep the BER within a prescribed range and adjust the modulation scheme accordingly.

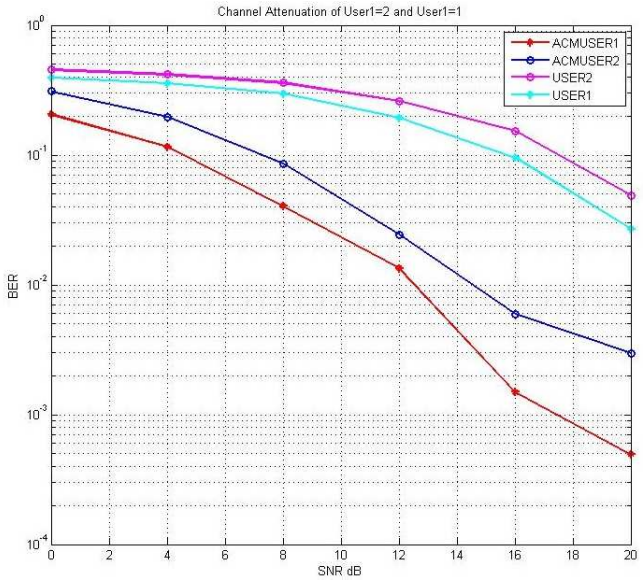

Figure 6 Comparison Results for users 1 and 2 with and without ACM and channel attenuation of 2 and 1 dB respectively.

The current graph represents a reversal of the previous one, where the values are comparable except for the distinction that user1 now has a channel attenuation of 2, while user2 maintains a value of 1. The behavior observed remains identical to that of the previous graph. This consistency arises from the utilization of a system that calculates the joint probability of both received signals, resulting in consistent outcomes. The behavior primarily relies on the properties of the channel, indicating that the receiver's response remains unchanged regardless of the number or position of the transmission antennas.

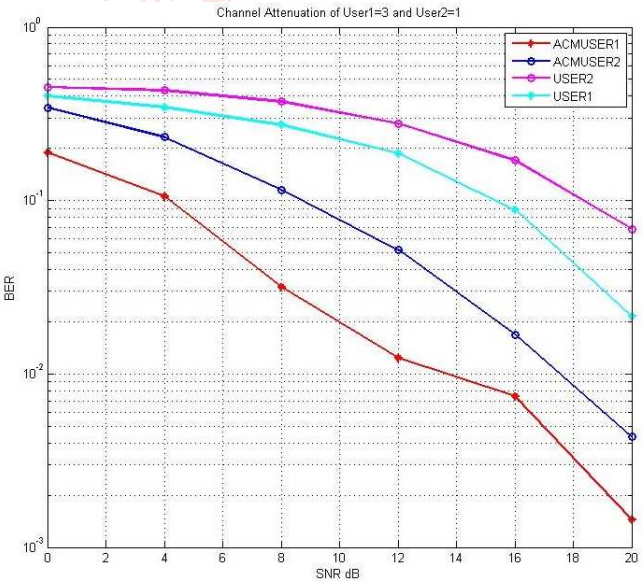

Figure 7 Comparison Results for users 1 and 2 with and without ACM and channel attenuation of 3 and 1 dB respectively.

Within this graph, we raise the channel attenuation of user1 to 3 while keeping the channel attenuation of user2 at 1. The behavior of user2 exhibits a higher bit error rate (BER), whereas user1 displays a lower BER with a more rapid decline. When compared to the

previous graph, where user2 had a channel attenuation of 1, the current graph demonstrates a steeper trend. Moreover, increasing the channel attenuation of user1 leads to a modification in the receiver properties, resulting in an overall reduction in the BER value.

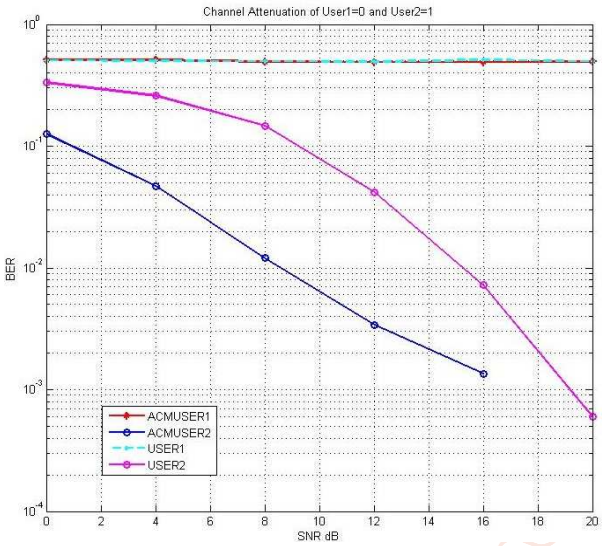

Figure 8 Comparison Results for users 1 and 2 with and without ACM and channel attenuation of 0 and 1 dB respectively.

To conduct a more comprehensive analysis, user1's channel attenuation is decreased to 0, while user2's attenuation remains at 1. The resulting outcome is notably distinct, as evident from the graph. For user1, both with and without adaptive coding and modulation (ACM), the bit error rate (BER) remains constant. This could be attributed to the receiver's inability to calculate the minimum distance, resulting in a consistent BER value. On the other hand, for user2, the graph abruptly terminates when ACM is employed. This observation necessitates further investigation to gain a deeper understanding of the system's behavior in this scenario.

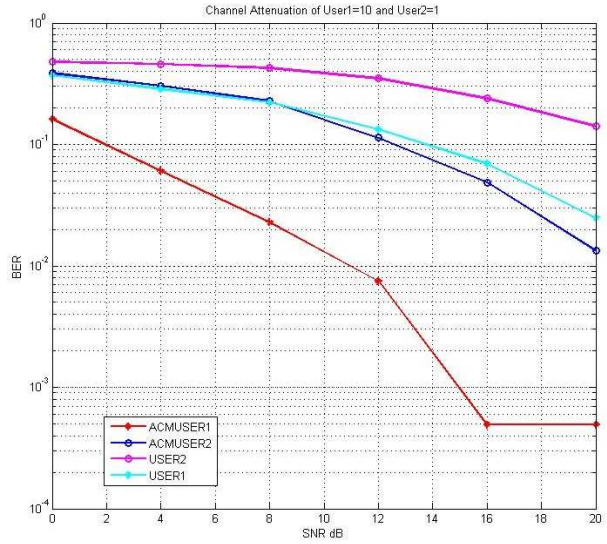

Figure 9 Comparison Results for users 1 and 2 with and without ACM and channel attenuation of 10 and 1 dB respectively.

Let us up the ante now by taking channel attenuation of user 1 as 10. When the difference in channel attenuation value is high the receiver sends back information to compensate for the BER and thus the BER of the other user, user2 in this case drastically increases. The BER of user1 is lower than in any of the previous cases.

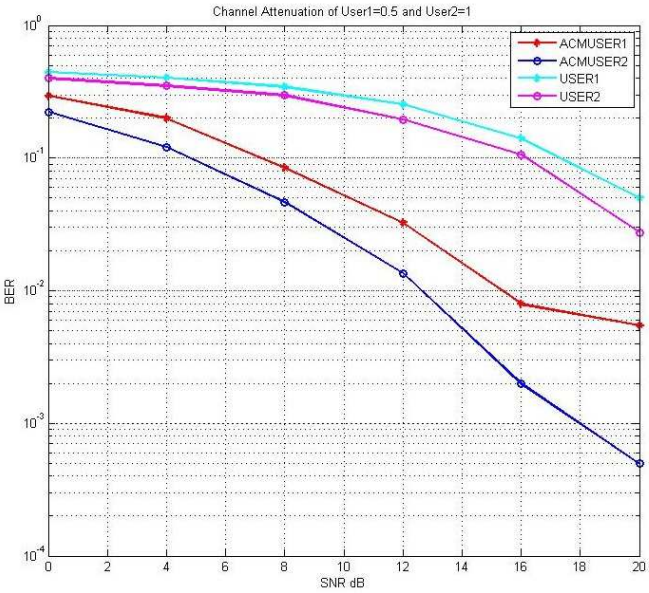

Figure 10 Comparison Results for users 1 and 2 with and without ACM and channel attenuation of 0.5 and 1 dB respectively.

The graph presents an intriguing observation. In this case, the channel attenuation for user1 is 0.5, which lies between the values of 0 and 1. Interestingly, the graph exhibits characteristics that closely resemble the scenario where the channel attenuation is set to 1. This implies that when the difference in channel attenuation is small, the disparity in the bit error rate (BER) values diminishes. However, the overall behavior remains consistent.

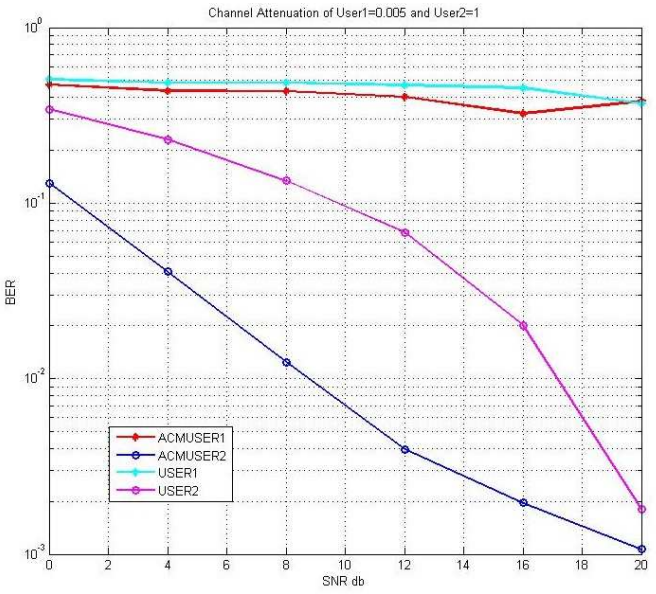

Figure 11 Comparison Results for users 1 and 2 with and without ACM and channel attenuation of 0.005 and 1 dB respectively.

By reducing user1's channel attenuation to 0.005, a different outcome is observed, lying between the bit error rate (BER) values of users with channel attenuations of 0 and 1. Both user1, with and without adaptive coding and modulation (ACM), maintain a relatively stable BER as observed in the case of channel attenuation 0. However, the second users display a more gradual decline in the graph. This suggests that the receiver is attempting to optimize channel utilization by striking a balance between the two channel attenuation values, aligning with our original objective.

When considering channel attenuation values of 1 for user1 and 0.1 for user2, the graph representing the multiple access spatial modulation (SM) case exhibits a slight decrease compared to its previous state. Consequently, the user with adaptive coding and modulation (ACM) aligns closely with it, especially in the scenario where the channel attenuation is set to 0.1.

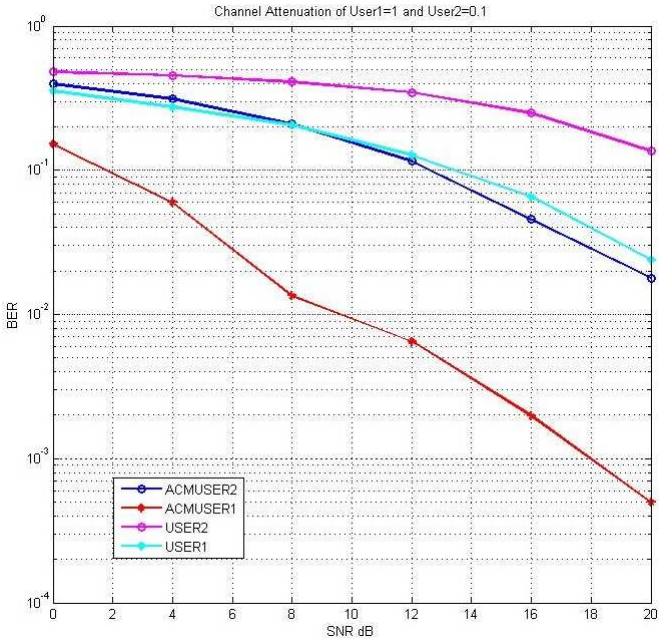

Figure 12 Comparison Results for users 1 and 2 with and without ACM and channel attenuation of 1 and 0.1 dB respectively.

V. CONCLUSION

We conducted a study on the performance of a multiple access spatial modulation system with adaptive coding and modulation (ACM). By implementing a maximum likelihood (ML) receiver in a Rayleigh fading channel, we successfully improved the system performance through ACM and code-division multiple access (CDMA). We examined the impact of varying channel attenuation values and the number of antennas on the bit error rate (BER). The results demonstrated a significant enhancement in BER with ACM compared to the absence of ACM and CDMA.

Furthermore, we investigated the BER of both users under different changes in channel attenuation. The receiver consistently exhibited similar performance characteristics for both users, which was a key consideration. To optimize the received signals, we employed the concept of joint probability**.**

References

[1] L. Lu, G. Y. Li, A. L. Swindlehurst, A. Ashikhmin, and R. Zhang, "An overview of massive MIMO: Benefits and challenges," IEEE J. Sel. Areas Commun., vol. 8, no. 5, pp. 742–758, Oct. 2014.

[2] J. G. Andrews, S. Buzzi, W. Choi, S. V. Hanly, A. Lozano, A. C. K. Soong, and J. C. Zhang, "What will 5G be?" IEEE J. Sel. Areas Commun., vol. 32, no. 6, pp. 1065–1082, Jun. 2014.

[3] V. W. Wong, R. Schober, D. W. K. Ng, and L.-C. Wang, Key technologies for 5G wireless systems. Cambridge university press, 2017.

[4] E. Dahlman, G. Mildh, S. Parkvall, J. Peisa, J. Sachs, Y. Seln, and J. Skld, "5G wireless access: Requirements and realization," IEEE Commun. Mag., vol. 52, no. 12, pp. 42–47, Dec. 2014.

[5] R. Mesleh, H. Haas, C. W. Ahn, and S. Yun, "Spatial modulation - a new low complexity spectral efficiency enhancing technique," in Proc. IEEE Int. Conf. Commun. Netw. in China, Beijing, China, Oct. 2006, pp. 1–5.

[6] R. Y. Mesleh, H. Haas, S. Sinanovic, C. W. Ahn, and S. Yun, "Spatial modulation," IEEE Trans. Veh. Technol., vol. 57, no. 4, pp. 2228–2241, Jul. 2018.

[7] M. D. Renzo, H. Haas, A. Ghrayeb, S. Sugiura, and L. Hanzo, "Spatial modulation for generalized MIMO: Challenges, opportunities, and implementation," Proc. IEEE, vol. 102, no. 1, pp. 56–103, Jan. 2014.

[8] M. Di Renzo, H. Haas, and P. M. Grant, "Spatial modulation for multiple- antenna wireless systems: A survey," IEEE Commun. Mag., vol. 49, no. 12, pp. 182–191, Dec. 2021.

[9] P. Yang, M. Di Renzo, Y. Xiao, S. Li, and L. Hanzo, "Design guidelines for spatial modulation," IEEE Commun. Surveys Tuts., vol. 17, no. 1, pp. 6–26, First quarter 2015.

[10] P. Yang, Y. Xiao, Y. L. Guan, K. V. S. Hari, A. Chockalingam,S. Sugiura, H. Haas, M. Di

Renzo, C. Masouros, Z. Liu, L. Xiao,S. Li, and L. Hanzo, "Single-carrier SM-MIMO: A promising design for broadband large-scale antenna systems," IEEE Commun. Surveys Tuts., vol. 18, no. 3, pp. 1687–1716, Third quarter 2016.

[11] A. Stavridis, S. Sinanovic, M. Di Renzo, and H. Haas, "Energy evalua- tion of spatial modulation at a multi-antenna base station," in Proc. IEEE Veh. Technol. Conf. (VTC Fall), Las Vegas, NV, USA, Sept. 2013, pp. 1–5.

[12] A. Stavridis, S. Sinanovic, M. Di Renzo, H. Haas, and P. Grant, "An energy saving base station employing spatial modulation," in Proc. IEEE Int. Workshop on Comput. Aided Modeling and Design of Commun. Links and Netw. (CAMAD), Barcelona, Spain, Sept. 2012, pp. 231–235.

[13] D. A. Basnayaka, M. Di Renzo, and H. Haas, "Massive but few active MIMO," IEEE Trans. Veh. Technol., vol. 65, no. 9, pp. 6861–6877, Sept. 2016.

[14] Y. Cui and X. Fang, "Performance analysis of massive spatial modulation MIMO in high-speed railway," IEEE Trans. Veh. Technol., vol. 65, no. 11, pp. 8925–8932, Nov. 2016.

[15] J. Jeganathan, A. Ghrayeb, L. Szczecinski, and A. Ceron, "Space shift keying modulation for MIMO channels," IEEE Trans. Wireless Commun., vol. 8, no. 7, pp. 3692–3703, Jul. 2019.

[16] M. D. Renzo, D. D. Leonardis, F. Graziosi, and H. Haas, "Space shift keying (SSK) MIMO with practical channel estimates," IEEE Trans. Commun., vol. 60, no. 4, pp. 998–1012, Apr. 2019.

[17] J. Choi, "Sparse signal detection for space shift keying using the Monte Carlo EM algorithm," IEEE Signal Process. Lett., vol. 23, no. 7, pp. 974–978, Jul. 2016.

[18] H. W. Liang, W. H. Chung, and S. Y. Kuo, "Coding-aided K-means clustering blind transceiver for space shift keying MIMO systems," IEEE Trans. Wireless Commun., vol. 15, no. 1, pp. 103–115, Jan. 2016.

[19] M. Di Renzo and H. Haas, "Improving the performance of space shift keying (SSK) modulation via opportunistic power allocation," IEEE Commun. Lett., vol. 14, no. 6, pp. 500–502, Jun. 2018.

[20] A. Younis, N. Serafimovski, R. Mesleh, and H. Haas, "Generalised spatial modulation," in Proc. Conf. Rec. 44th Asilomar Conf. Signals, Syst. Comput, Pacific Grove, CA, USA, Nov. 2019, pp. 1498–1502.

[21] Fu, C. Hou, W. Xiang, L. Yan, and Y. Hou, "Generalised spatial modulation with multiple active transmit antennas," in Proc. IEEE Globecom Workshops (GC Wkshps), Miami, FL, USA,Dec. 2019, pp. 839–844.

[22] J. Wang, S. Jia, and J. Song, "Generalised spatial modulation system with multiple active transmit antennas and low complexity detection scheme," IEEE Trans. Wireless Commun., vol. 11, no. 4, pp. 1605–1615, Apr. 2018.

[23] B. Zheng, X. Wang, M. Wen, and F. Chen, "Soft demodulation algo- rithms for generalized spatial modulation using deterministic sequentialmonte carlo," IEEE Trans. Wireless Commun., vol. 16, no. 6, pp. 3953– 3967, Jun. 2017.

[24] R. Mesleh, S. S. Ikki, and H. M. Aggoune, "Quadrature spatial modu- lation," IEEE Trans. Veh. Technol., vol. 64, no. 6, pp. 2738–2742, Jun. 2015.

[25] Y. Bian, X. Cheng, M. Wen, L. Yang, H. V. Poor, and B. Jiao, "Differential spatial modulation," IEEE Trans. Veh. Technol., vol. 64, no. 7, pp. 3262–3268, Jul. 2015.

[26] N. Ishikawa and S. Sugiura, "Unified differential spatial modulation", IEEE Wireless Commun. Lett., vol. 3, no. 4, pp. 337–340, Aug. 2014.

[27] M. Wen, X. Cheng, Y. Bian, and H. V. Poor, "A low-complexity near- ML differential spatial modulation detector," IEEE Signal Process. Lett., vol. 22, no. 11, pp. 1834–1838, Nov. 2015.

[28] L. Yang, "Transmitter preprocessing aided spatial modulation for multiple-input multiple-output systems," in Proc. IEEE Veh. Technol. Conf. (VTC Spring), Yokohama, Japan, May 2021, pp. 1–5.

[29] A. Stavridis, S. Sinanovic, M. Di Renzo, and H. Haas, "Transmit precod- ing for receive spatial modulation using imperfect channel knowledge," in Proc. IEEE Veh. Technol. Conf. (VTC Spring), Yokohama, Japan, May 2021, pp. 1–5.

[30] R. Zhang, L. Yang, and L. Hanzo, "Generalised pre-coding aided spatial modulation," IEEE Transactions on Wireless Communications, vol. 12, no. 11, pp. 5434–5443, Nov. 2018.

[31] J. Jeganathan, A. Ghrayeb, and L. Szczecinski, "Generalized space shift keying modulation for MIMO channels," in Proc. IEEE Int. Symp. Personal, Indoor, Mobile Radio Commun. (PIMRC), Cannes, France, Sept. 2018, pp. 1–5.

[32] E. Basar, M. Wen, R. Mesleh, M. D. Renzo, Y. Xiao, and H. Haas, "Index modulation techniques for next-generation wireless networks," IEEE Access, vol. 5, pp. 16 693–16 746, 2017.

[33] B. Zheng, M. Wen, F. Chen, N. Huang, F. Ji, and H. Yu, "The K-best sphere decoding for soft detection of generalized spatial modulation," IEEE Trans. Commun., vol. 65, no. 11, pp. 4803–4816, Nov. 2017.

[34] P. Yang, Y. Xiao, Y. Yu, and S. Li, "Adaptive spatial modulation for wireless MIMO transmission systems," IEEE Commun. Lett., vol. 15, no. 6, pp. 602–604, Jun. 20119.

[35] P. Yang, Y. Xiao, L. Li, Q. Tang, Y. Yu, and S. Li, "Link adaptation for spatial modulation with limited feedback," IEEE Trans. Veh. Technol., vol. 61, no. 8, pp. 3808–3813, Oct. 2020.